# Identification of Marine Terraces Through Digital Elevation Maps in the Shikoku Region of Japan

Rachel Bailey[1] and Yosuke Aoki[2]

[1]Department of Physics, College of William & Mary
[2]Department of Earth Sciences, University of Tokyo

September 2024

**Abstract**

Methods have been proposed for the identification of marine terraces without field surveys involving digital elevation maps and K-means cluster analysis [2]. This method has been tested in one area of Japan, however its applicability to other regions has yet to be examined. The Shikoku region of Japan is well known for marine terrace formations, and they have been previously identified and categorized [3]. In this study, new methods are applied to attempt to replicate these identifications without the assistance of field survey data. Individual cross-sections replicating those already studied were taken and compared to previous literature. DEMs and algorithms were able to identify many terraces with significant accuracy, however algorithms must be refined in the event that many cross-sections perpendicular to the coast are taken to avoid false positive terrace identification. Overall, results of analysis are promising for their use in machine learning and cluster analysis as a method of identifying marine terraces.

## 1 Introduction

### 1.1 Background Information

Marine terraces are step-like topography present along coastlines that are artifacts of paleo-earthquakes. They often come in sets, representing an area with frequent (even regular) large-magnitude earthquakes on one fault line. Geometrically, they appear as sequences of short, steep inclines of paleo-sea cliffs perpendicular to coastlines followed by stretches of flatter land (terrace platforms).

The study of their age in combination with tectonic uplift can provide insight toward improving earthquake early warning systems and natural disaster prevention.

### 1.2 Technical References

Historically, the identification of marine terraces is often completed through field surveys, including core samples. Newer methods involve the comparison of digital elevation maps to these field surveys as verification of previous data, like that which will be discussed in this article [5][1]. However, a newer method that has been proposed utilizes the application of K-means clustering to locate marine terrace formations and group them without the use of field surveys [2].

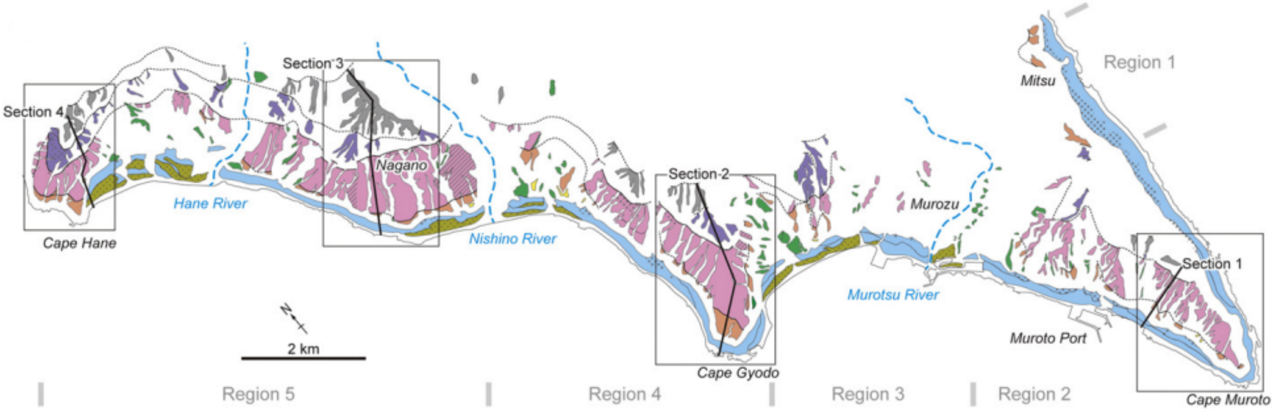


Figure 1: Graphic from T. Matsu'ura, 2015 showcasing Regions 1-5 of the Muroto Peninsula [3].

K-means clustering is considered an unsupervised machine learning method that assesses the potential for patterns within seemingly random datasets, grouping data via given algorithms [4]. Through the use of this method and other formulae to isolate the location of terraces, groups of terraces can be identified.

### 1.3 Present Region of Interest

The methods proposed have not yet been applied to the Shikoku region of Japan along the Muroto Peninsula, already known to be host to a stretch of marine terraces identified through field surveys [3][6]. Categorized as the Hane-Saki terraces (H1 and H2), the Muroto–Misaki terraces (M1, M2, and M3), and the lower terraces (L), the marine terraces of the Shikoku region date mainly from the Late-Quaternary period, though the lower terraces and M3 emerged during the Holocene.

As the given data set of digital elevation maps have the elevation of 0m at approximately −40m below the known sea level of the region, this has been corrected during data analysis. However, it is not known at this time whether this estimate is exact, and thus the applied normalization may be inaccurate to the order of ±10m. The true DEM elevation of sea level within this region should be verified upon the progression of this research.

## 2 Mathematics Foundation

In an effort to locate terraces to eventually be analyzed with K-means clustering, first a cross-section must be taken perpendicular to the coastline. Following this, a smoothing function must be applied to convert the elevation data into a monotonically increasing function. Each horizontal point $y'$ is then evaluated via

$$H(y'+r) > H(y') + dz \tag{1}$$

with $r$ being a distance inland, and $dz$ a distance upwards in elevation. The inequality establishes that if the elevation at a point $r$ away inland is greater than the elevation at point $y'$ in addition to a height $dz$, then that $y'$ represents the point inland where a terrace begins. In other words, if an elevation $y'$ satisfies the inequality, it is considered the location of a terrace inner edge.

It is important to note that these values are determined by setting a general scope of analysis, choosing two elevations $H1$ and $H2$ and recording the distance $L$ horizontally between the two points to estimate the average slope of area and isolate slope oddities ascribed to terrace formations. From these values, $r$ and $dz$ are determined as

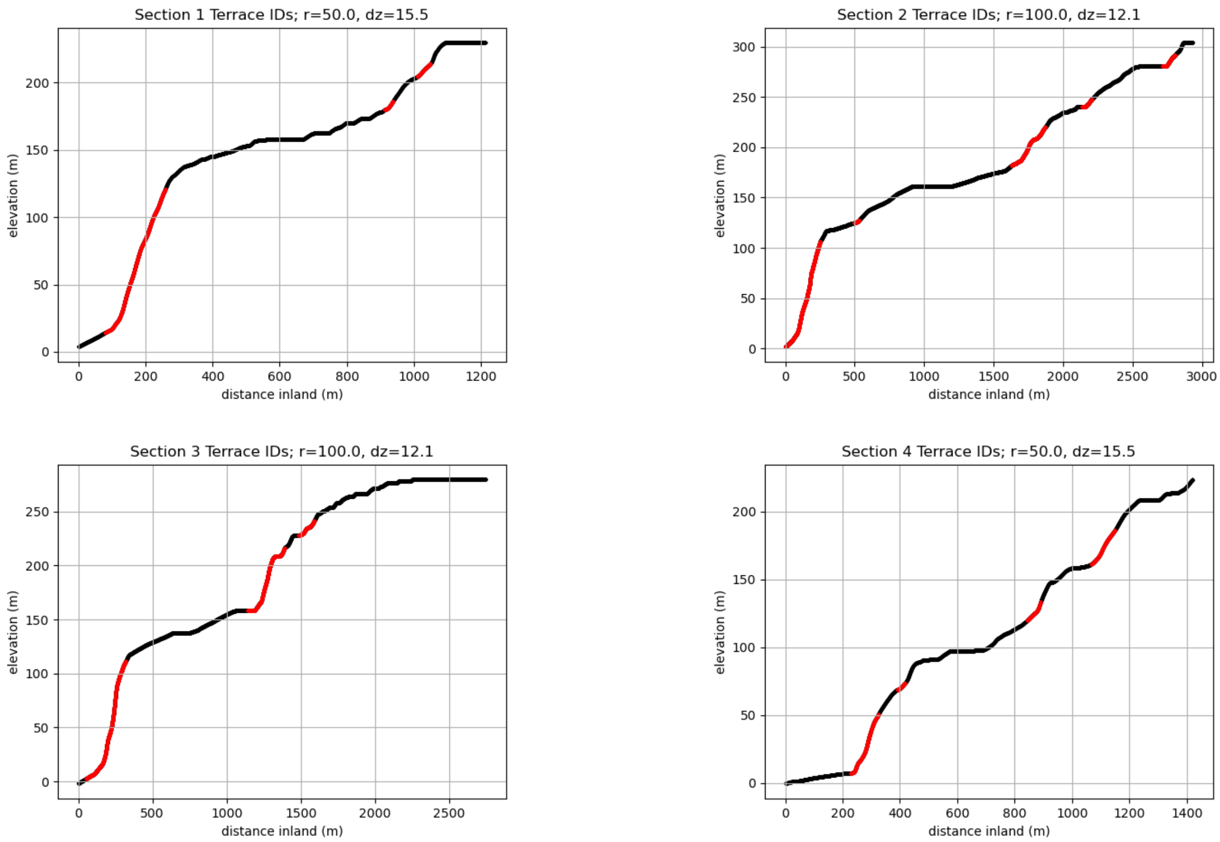


Figure 2: Vertical cross-sections of Sections 1-4 from Figure 1 partway through terrace inner edge identification. A smoothing function has been applied to the true cross-sections to create monotonically increasing geometry, and highlighted in red are areas identified with sufficient increase to satisfy Equation 1.

$$r = \mathbf{q}L \tag{2}$$

and

$$dz = r\tan(\theta) \tag{3}$$

The value of $dz$ is in part determined by the value of $r$, however the angle $\theta$ is determined by $H1$, $H2$, and $L$ through their relation to $\phi$, the average angle of coastal elevation increase. These angles are established as

$$\phi = \frac{H2 - H1}{L} \tag{4}$$

and

$$\theta = \mathbf{p}\phi \tag{5}$$

Note at this point the values $p$ and $q$. These are what truly determine topography identifiable as marine terraces in a region and can be fine-tuned to the area of interest. The Boso Peninsula is a smaller area than the Muroto Peninsula, therefore $p$ and $q$ were increased for this study, scaled differently for areas that were smaller than others.

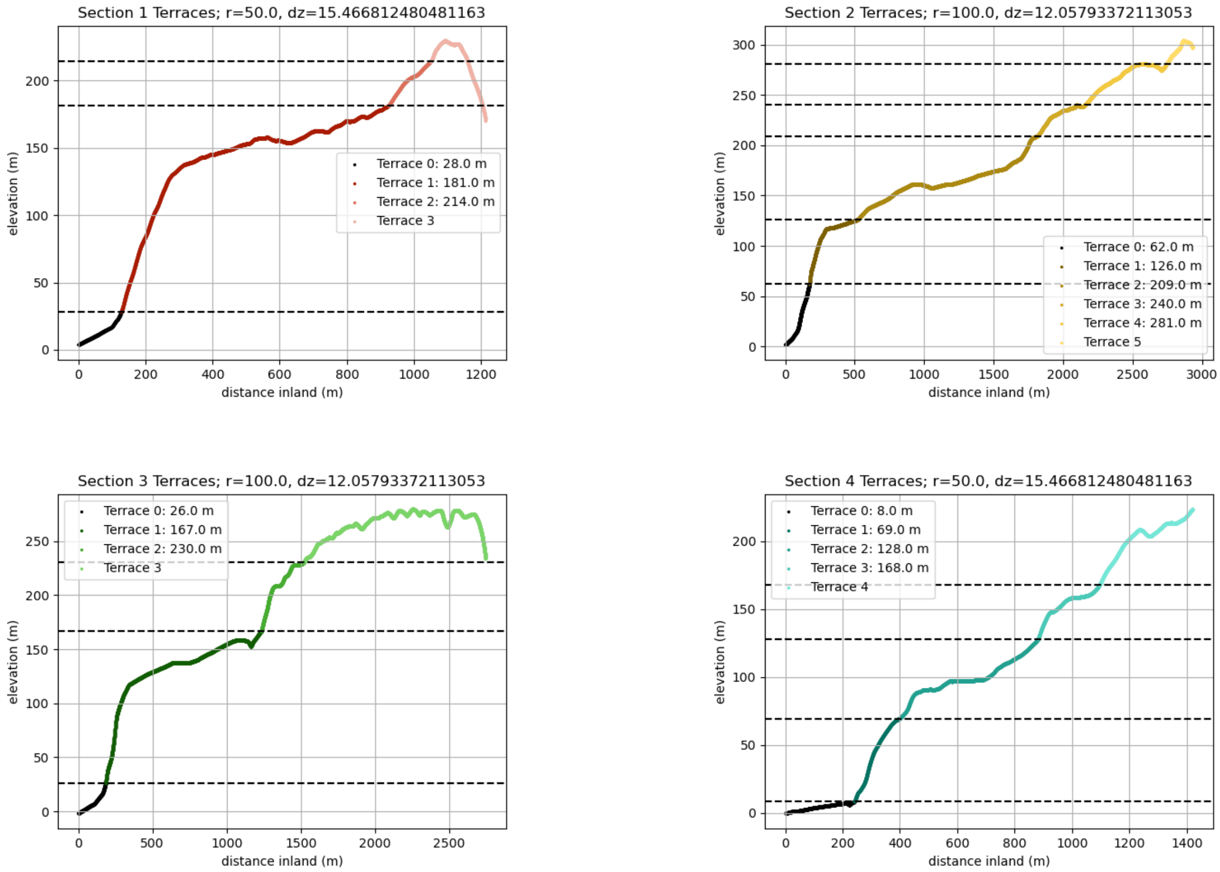


Figure 3: Identified terrace inner edges in Sections 1-4 from Figure 1. Terrace 0 in all graphs represents the transition from beach to terrace formations (limited diagnostic accuracy, as seen in Section 2). Comparison between inner edges and previous literature can be found in Table 1.

Once distances inland $y'$ are identified as possible terrace inner edges, the location of the inner edge within a grouping of $y'$s is selected as the point with the largest curvature $\kappa$, defined as

$$\kappa = -\frac{2H(x) - H(x-\mathbf{s}) - H(x+\mathbf{s})}{\mathbf{s}^2} \tag{6}$$

with $s$ being the search radius. $s$ in previous literature is defined as $r$ and is redefined here to avoid confusion with $r$ in Equation 1 [2]. This parameter was also scaled for the Muroto Peninsula to a value of 10m.

## 2.1 Implementation

To test the accuracy of the proposed mathematics, identical cross-sections to those taken previously were selected from DEMs and terraces were identified through Formulas 1 and 6. The output elevations for marine terrace inner edges were then compared to those determined in previous work [3]. Figure 2 is of Sections 1-4 shown in Figure 1 partway through terrace identification (prior to the identification of maximum curvature points). These graphs display cross-sections

Terrace Inner Edge Elevations: Prior Analysis and New

| Section | M2 | | M1 | | H2 | | H1 | |
|---|---|---|---|---|---|---|---|---|
| | Prior (m) | New (m) | Prior (m) | New (m) | Prior (m) | New (m) | Prior (m) | New (m) |
| 1: Cape Muroto | 141 | - | 182 | 181 | - | 214 | - | - |
| 2: Cape Gyodo | 131 | 126 | 190 | 209* | 264 | 240* | 286 | 281 |
| 3: Nagano | 116 | - | 168 | 167 | 233 | 230 | (H1) | (H1) |
| 4: Cape Hane | 75 | 69 | 118 | 128 | 164 | 168 | (H1) | (H1) |

Table 1: A comparison of terrace inner edge identifications from a previous study and the identifications made in current work. Data reported with asterisks are representative of those that do not fall within the reported window of elevations for the terrace with which they most align given a ±5m margin of error. Measurements are reported in meters and errors of ±5m are present in all current measurements. Prior terrace inner edge elevations reported by T. Matsu'ura, found in Table 8 [3].

smoothed to be monotonically increasing with regions satisfying Equation 1 highlighted in red.

In Figure 3, elevations of marine terrace inner edges are identified for Sections 1-4, and their elevations are compared to those established in previous work in Table 1. Error on depicted elevations is reliant upon the error of the DEMs, thus an error in elevation of ±5m and a horizontal error of ±0.1m.

## 3 Cross-Section Analysis

From Figure 3, it is evident that the script designed during this study still has difficulty identifying terrace M2 from its failure to do so in Section 1 and 3, however it has been noted that this inner edge does not have a prominent slope differential [3]. However, while previous cross-sections of Section 1 did not identify terrace

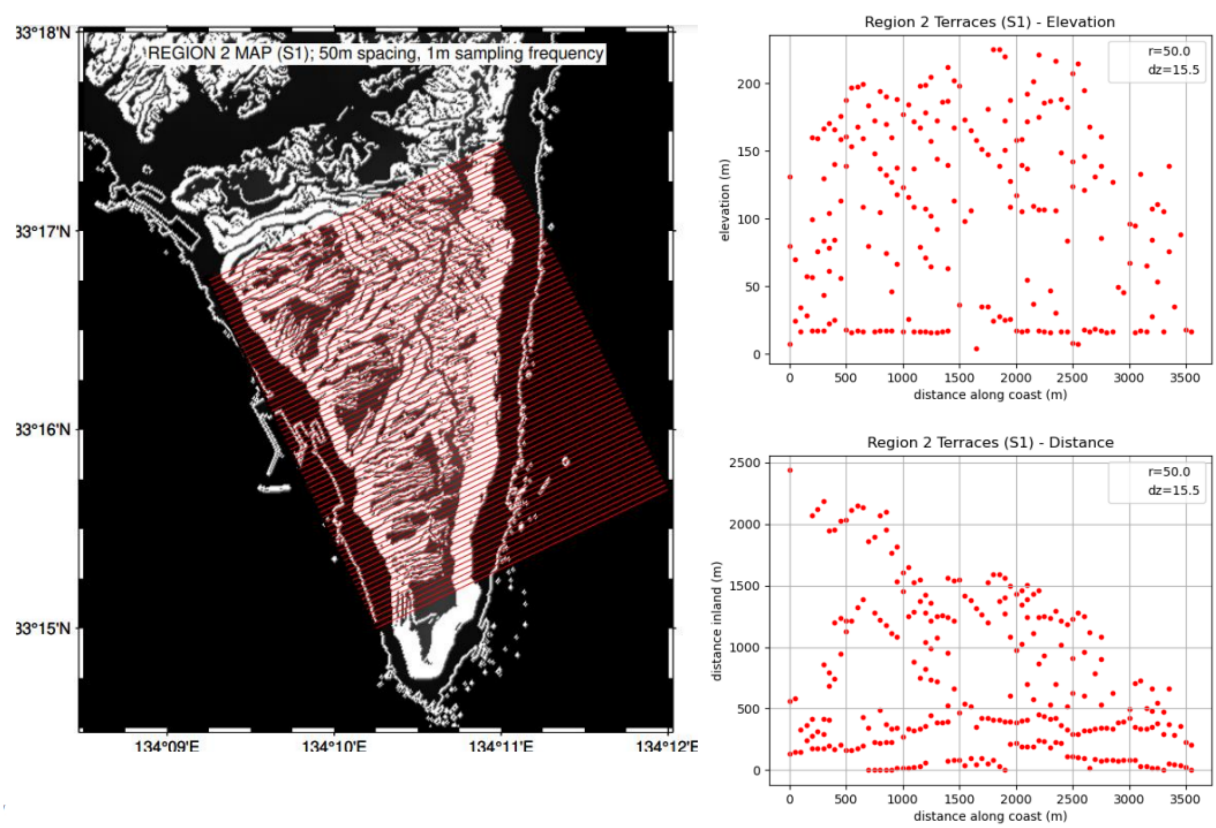


Figure 4: **Left:** A digital elevation map of Cape Muroto to the Murozu River (Region 2), with areas of lower elevation gradient shown in black and cross-sections shown in red. Cross-sections had a spacing of 50m between each other and a sampling frequency of every 1m. Inner terrace edges identified within these cross-sections via Equations 1 and 6 correspond directly with data shown in the elevation and distance plots pictured on the right. **Right-Top:** Plot of distance along coastline versus elevation of identified terrace inner edge. Groupings in elevation are moderately apparent, making the sample a candidate for the K-means clustering method. **Right-Bottom:** Plot of distance along coastline against distance inland along cross-section of terrace inner edges. Terrace units are geographically visible in the dataset.

H2, a terrace is noted in Figure 3, Section 1 at an elevation of $214 \pm 5$m, which is within the range proposed for H2 in the Cape Muroto region [3].

Table 1 displays that most terrace inner edge identifications done in this study fall within the accepted range of inner edges previously proposed, with some notable outliers in M1 and H2 of Section 2. However, review of the cross-sections reveals terrace platform and paleo-sea cliff geometry present at all newly proposed inner edges, despite their failure to fall within the accepted band. Additional error could be present from the use of an estimation of sea level, as all terrace elevation data except M1 in Section 2 and H2 in Section 4 are lower than expected.

To test the efficacy of this method when taking other cross-sections that may approach terrace formations obliquely, cross-sections of constant length were taken at 50m intervals perpendicular to a line drawn along the coast. We took these over Regions 2, 4, 5, and 6 to encompass areas represented in the Sections analyzed, and results are plotted in Figures 4-7. Horizontal error increased to $\pm 1$m to lessen computational workload by sampling every 1m horizontally along a cross-section instead of every 0.1m. Figures 5-7 can be found in the appendix.

Figure 4 can act as an example for interpretation of Figures 5-7, as their methods of generation were near identical. While clear groupings in the elevation map are not present, general trends match previously reported elevations of inner terrace edges in the region [3]. Additionally, the distance plot and associated digital elevation map indicate that inner angles identified by Equations 1 and 6 are occurring in areas of high gradient on the DEM. These trends are also evident in Figures 5-7. All regions (most notably Region 5/6, displayed in Figure 7) show significant potential as candidates for K-means cluster analysis.

## 4 Conclusions and Discussion

Overall, data suggests that the Shikoku Region of Japan is an acceptable candidate for the application of K-means clustering for the purpose of marine terrace identification, as seen by the production of elevation and distance plots along cross-sections in the area.

One aspect that could improve the accuracy of the results is altering the current smoothing function. The elevation geometry created in an attempt to smooth data to be monotonically increasing allows for sharp angles along the direction of increasing elevation. This builds a shape falsely recognizable to the algorithm as a terrace inner edge. Improvements to the architecture of this smoothing function would greatly aid in removing false positive data.

An approach to avoiding oblique marine terrace analysis is to utilize DEMs of the gradient of the region and take cross-sections that are perpendicular to evident terrace slope, however this method is a bit reflexive, as to do this best it must be known that a terrace is present in the first place. Thus, the ideal method to improving terrace identification is through honing the smoothing function and narrowing down ideal $p$ and $q$ values to produce the most representative version of Equation 1 for the region in question. Attempts at utilizing K-means clustering analysis can follow these improvements.

## References


[1] C. J. Bowles and E. Cowgill. Discovering marine terraces using airborne lidar along the mendocino-sonoma coast, northern california. *Geosphere*, 8(2):386–402, 2012.

[2] J. Komori, R. Ando, and M. Shishikura. Cluster analysis of marine terraces and quantitative seismotectonic interpretation of the boso peninsula, central japan. *Journal of Geophysical Research: Solid Earth*, 125(8):e2019JB019211, 2020.

[3] T. Matsu'ura. Late quaternary uplift rate inferred from marine terraces, muroto peninsula, southwest japan: Forearc deformation in an oblique subduction zone. *Geomorphology*, 234:133–150, 2015.

[4] C. Piech and A. Ng. K means. *Stanford CS221*, 2013. `https://stanford.edu/~cpiech/cs221/handouts/kmeans.html` (accessed: 09.05.24).

[5] A. T. Scott and N. Pinter. Extraction of coastal terraces and shoreline-angle elevations from digital terrain models, santa cruz and anacapa islands, california. *Physical Geography*, 24(4):271–294, 2003.

[6] T. Yoshikawa, S. Kaizuka, and Y. Ota. Mode of crustal movement in the late quaternary on the southeast coast of shikoku, southeastern japan. *Geogr. Rev. Jpn*, 37:627–648, 1964. (in Japanese, with English Abstr.).

# A Regional Cross-Section Swaths, Regions 4-6

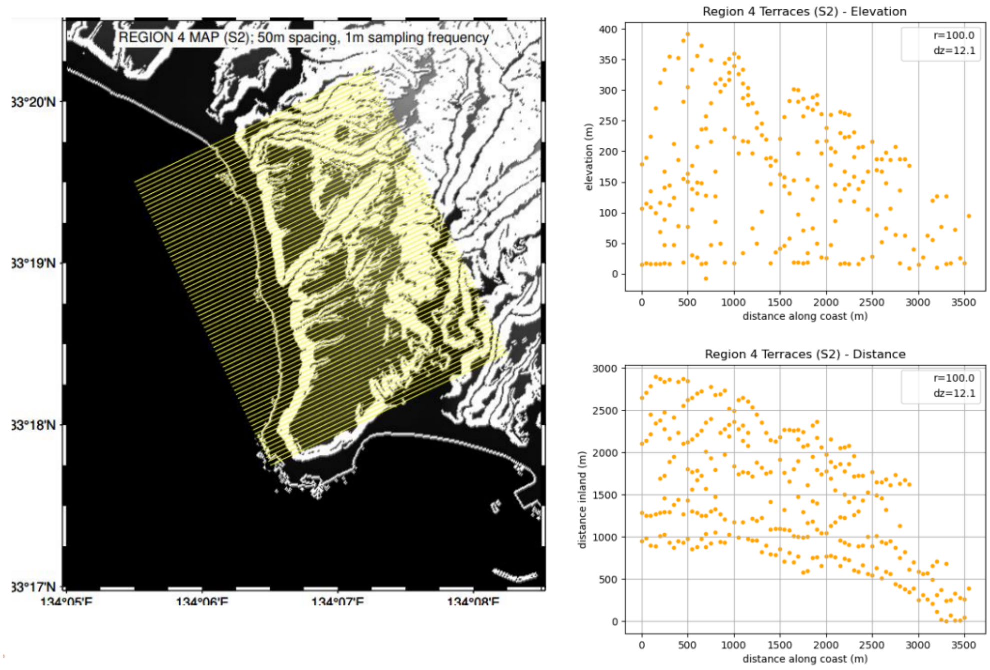


Figure 5: **Left:** A digital elevation map of Cape Gyodo to the Nishino River (Region 4), with areas of lower elevation gradient shown in black and cross-sections shown in yellow. Formatting identical to Figure 4. **Right-Top:** Plot of distance along coastline versus elevation of identified terrace inner edge. Groupings in elevation are moderately apparent, making the sample a candidate for the K-means clustering method. **Right-Bottom:** Plot of distance along coastline against distance inland along cross-section of terrace inner edges. Terrace units are geographically visible in the dataset.

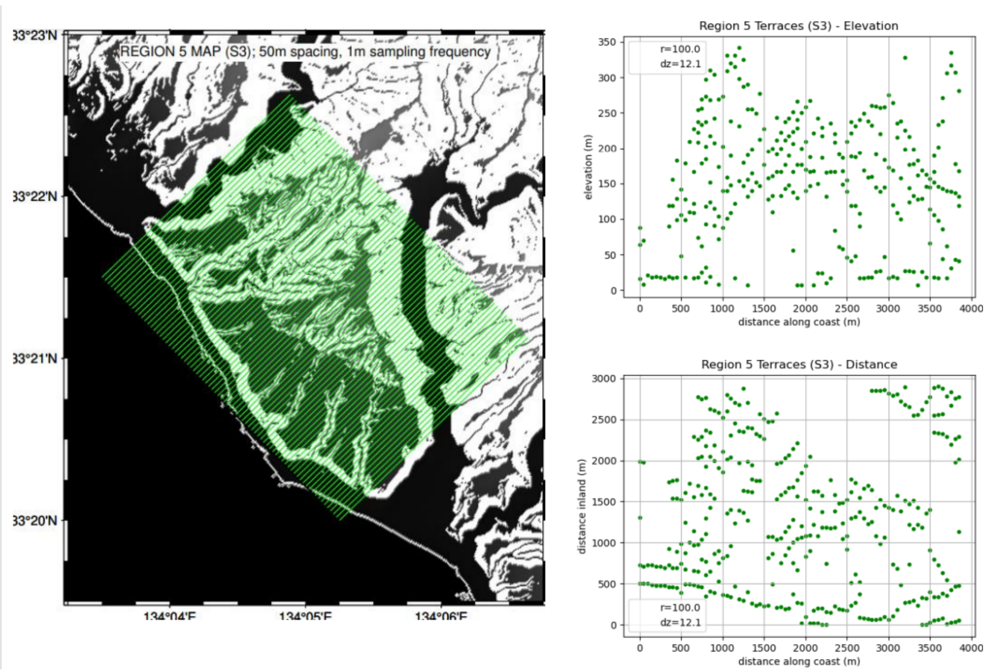


Figure 6: **Left:** A digital elevation map of the Nishino Rive to the Hane River (Region 5), with areas of lower elevation gradient shown in black and cross-sections shown in green. Formatting identical to Figure 4. **Right-Top:** Plot of distance along coastline versus elevation of identified terrace inner edge. Groupings in elevation are moderately apparent, making the sample a candidate for the K-means clustering method. **Right-Bottom:** Plot of distance along coastline against distance inland along cross-section of terrace inner edges. Terrace units are geographically visible in the dataset.

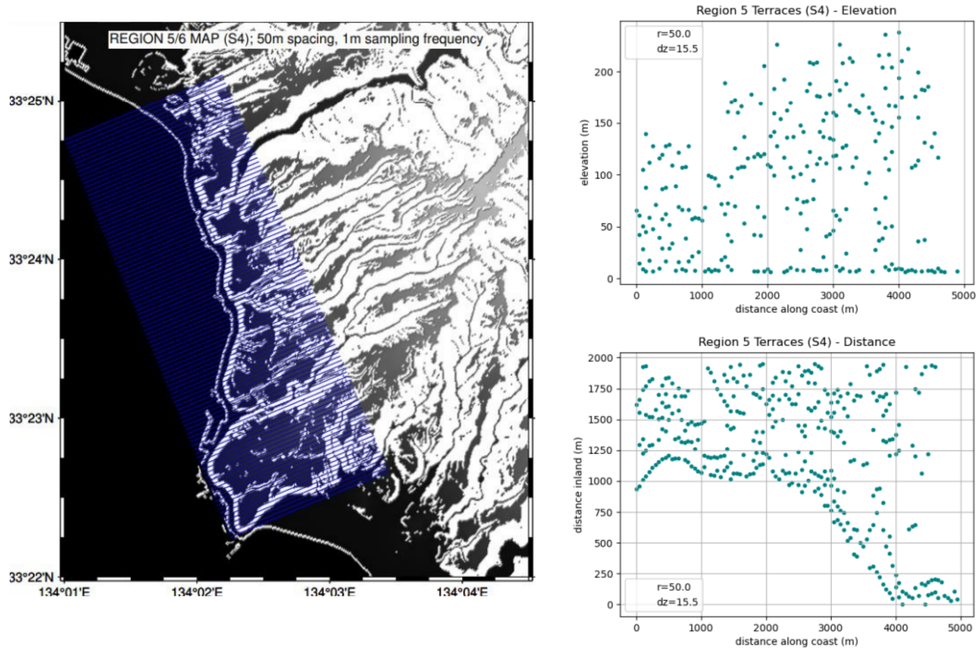


Figure 7: **Left:** A digital elevation map of the Hane River to Cape Oyama (Region 5/6), with areas of lower elevation gradient shown in black and cross-sections shown in blue. Formatting identical to Figure 4. **Right-Top:** Plot of distance along coastline versus elevation of identified terrace inner edge. Groupings in elevation are moderately apparent, making the sample a candidate for the K-means clustering method. **Right-Bottom:** Plot of distance along coastline against distance inland along cross-section of terrace inner edges. Terrace units are geographically visible in the dataset.

| Region | H1 (MIS 7 or 9?) & H2 (MIS 7) | | M1 (MIS 5e) | | M2 (MIS 5c) | |
|---|---|---|---|---|---|---|
| | Elevation (m) | Uplift rate (m ky$^{-1}$) | Elevation (m) | Uplift rate (m ky$^{-1}$) | Elevation (m) | Uplift rate (m ky$^{-1}$) |
| 1 Mitsu | | | | | 117–132 | 1.3–1.5 |
| 2 Muroto–Murozu River | 189–229 | 0.8–1.3 | 164–182 | 1.2–1.6 | 119–141 | 1.3–1.6 |
| 3 Murozu River–Cape Gyodo | 190–218 | 0.8–1.2 | 126–143 | 0.9–1.2 | 109–119 | 1.2–1.4 |
| 4 Cape Gyodo–Nishino River | 264–308 | 1.1–1.5 | 165–192 | 1.2–1.7 | 119–142 | 1.3–1.6 |
| 5 Nishino River–Cape Hane | 159–276 | 0.7–1.5 | 102–178 | 0.7–1.5 | 67–113 | 0.8–1.3 |
| 6 Cape Hane–Cape Oyama | 91–276 | 0.4–1.5 | 60–118 | 0.4–1.0 | 40–81 | 0.5–1.0 |
| 7 Cape Oyama–Wajiki River | 86–182 | 0.4–1.0 | 49–78 | 0.3–0.7 | 31–41 | 0.4–0.5 |
| 8 Wajiki River–Koso River | 64–95 | 0.3–0.6 | 34–74 | 0.2–0.6 | 19–32 | 0.3–0.4 |

Figure 8: Table of terrace inner edges from T. Matsu'ura [3]. The elevation windows for Regions 2, 4, 5, and 6 are compared to elevations calculated in this study in Table 1.